



HAL
open science

Tailored therapeutic release from polycaprolactone-silica hybrids for the treatment of osteomyelitis: antibiotic rifampicin and osteogenic silicates

Lukas Gritsch, Henri Granel, Nicolas Charbonnel, Edouard Jallot, Yohann Wittrant, Christiane Forestier, Jonathan Lao

► To cite this version:

Lukas Gritsch, Henri Granel, Nicolas Charbonnel, Edouard Jallot, Yohann Wittrant, et al.. Tailored therapeutic release from polycaprolactone-silica hybrids for the treatment of osteomyelitis: antibiotic rifampicin and osteogenic silicates. *Biomaterials Science*, 2022, 10 (8), pp.1936-1951. 10.1039/d1bm02015c . hal-04056659

HAL Id: hal-04056659

<https://hal.science/hal-04056659>

Submitted on 19 Jun 2023

HAL is a multi-disciplinary open access archive for the deposit and dissemination of scientific research documents, whether they are published or not. The documents may come from teaching and research institutions in France or abroad, or from public or private research centers.

L'archive ouverte pluridisciplinaire **HAL**, est destinée au dépôt et à la diffusion de documents scientifiques de niveau recherche, publiés ou non, émanant des établissements d'enseignement et de recherche français ou étrangers, des laboratoires publics ou privés.

1 **Dual therapeutic tailored release from organic/inorganic hybrids: antimicrobial rifampicin and**
2 **osteogenic silicates.**

3 Lukas Gritsch^{1,*}, Henri Granel², Edouard Jallot¹, Yohann Wittrant², Christiane Forestier³ and Jonathan Lao¹

4 **Affiliations**

5 ¹ Laboratoire de Physique de Clermont, UMR CNRS 6533, Université Clermont Auvergne, 4 avenue Blaise
6 Pascal, 63178 Aubière, France

7 ² Unité de Nutrition Humaine UMR 1019 INRAE, Université Clermont Auvergne, 28 place Henri-Dunant,
8 63001 Clermont-Ferrand, France

9 ³ Université Clermont Auvergne, CNRS, LMGE, F-63000 Clermont–Ferrand, France

10 *** Corresponding author**

11 **Lukas Gritsch, e-mail: lukas.gritsch@clermont.in2p3.fr**

12 Laboratoire de Physique de Clermont, UMR CNRS 6533

13 Université Clermont Auvergne

14 4 avenue Blaise Pascal

15 63178 Aubière

16 France

1 **1 Introduction**

2 Osteomyelitis is among the most complex conditions encountered in orthopedic surgery and bone
3 reconstruction. It is defined as a bone tissue destructive inflammatory process caused by a bacterial infection. It
4 can be acute, characterized by soft tissue edema, pus formation and locally decreased blood supply, or chronic,
5 with formation of areas of bone necrosis (*sequestra*) that increase infection recurrence^[1,2]. Gram-positive strains
6 are most commonly involved, with a significant predominance of *Staphylococcus* and *Streptococcus* genera. In
7 particular, several reports identified *Staphylococcus aureus* as the major responsible worldwide, appearing in
8 50-70% of tested clinical isolates^[3-5]. Several mechanisms can lead to the onset of an infection, including
9 hematogenous, post-traumatic, local spread from contiguous outbreak, peri-operative colonization and
10 prosthesis/implant contamination (e.g., periprosthetic joint infection, PJI)^[6]. Treatment includes a combination
11 of tissue debridement, intense local antibiotic therapies^[7-9] and the implantation of a suitable graft when
12 necessary^[1,6]. The long-term outcome

13 of the procedure can be very challenging. In particular, the optimization of debridement is considered to be the
14 cornerstone of a successful treatment: since pathological tissues are poorly vascularized, their thorough removal
15 is of chief importance for the antibiotics to be effective and to reduce bone ischemia^[6]. However, high
16 debridement means high invasiveness and possibly longer prognosis. Reducing it could preserve the structural
17 integrity of bone, but at the cost of increasing the risk of recurrence^[1,10]. In any case, even with optimized
18 debridement, the treatment of osteomyelitis frequently results in significant bone defects that need tailored
19 medical care^[6]. In addition, infection sites are typically rich in cytokines (e.g., tumor necrosis factor or
20 interleukin-1). These biomolecules are strong osteolytic promoters and can hinder bone healing, even following
21 a successful intervention^[11,12].

22 The close relationship between osteomyelitis and bone defects is a strong drive for the development of novel
23 approaches and materials designed to improve bone healing and reduce the risk of infection relapse. A properly
24 engineered biomaterial should not only fill the bone defect but also improve regeneration and fend off possible
25 threats. In other words, it should be both antibacterial and osteostimulative. Driven by the promise of better
26 bone reconstruction, research in the field is investigating many candidate approaches, including drug-loaded
27 synthetic polymers (e.g., polylactic acid, polyglycolic acid), composites and hydroxyapatites, silver-based
28 nanotechnologies, quaternary chitosan and therapeutic ion releasing bioactive glasses^[13,14]. However, despite
29 their promising results in the laboratory, most of these technologies still lack significant clinical data to confirm
30 their efficacy. To date, no commercial product has been successfully launched yet^[15]. Currently, the gold
31 standard for bone defect management is the use of gentamicin-impregnated polymethylmethacrylate (PMMA)
32 cements^[16]. This technology, however, has several drawbacks, including: (i) the non-degradability and possible
33 toxicity of PMMA, (ii) the thermal degradation of gentamicin during cement setting and (iii) its inadequately
34 fast pharmacokinetics (i.e., burst release of 80-90% of the drug within 5 minutes)^[1,3,15]. Better results in terms of
35 drug delivery were recently obtained using bioresorbable calcium sulphate bone cements (CSCs) as carriers,
36 giving rise to new alternative possibilities in the treatment of osteomyelitis^[16,17]. Gentamicin, vancomycin and
37 tobramycin are the main antibiotics successfully used in conjunction with CSCs^[18]. Although desirable,
38 however, the high reactivity and rapid bioresorbability of CSCs is also a key limitation. The resorption rate is
39 too high to grant sufficient bone healing and CSCs are quickly hydrolyzed in the body (in 6 to 12 weeks)^[18]. In

1 addition, the fast resorption of CSCs was associated with wound serous exudate^[19]. Their mechanical properties
2 are also quite poor^[1], offering very limited structural support to the tissue. Generally speaking, both PMMA and
3 CSC offer a sufficient performance to tackle the problem, but also significant drawbacks. They have poor
4 pharmacokinetics and a very low regeneration potential. Furthermore, they are mostly used in conjunction with
5 very common, broad-spectrum antibiotics (e.g., gentamicin). The clinical need for new materials against
6 osteomyelitis remains therefore a pressing issue, with orthopedic surgeons still having few options available
7 whenever looking for antibacterial and osteostimulative bone fillers^[13].

8 In previous studies, class I polycaprolactone/bioactive glass (PCL/BG) hybrids were successfully synthesized
9 and characterized to be applied for the regeneration of bone defects^[20,21]. Organic/inorganic (O/I) hybrids are a
10 family of single-phase materials formed by a network of organic and inorganic moieties combined at the
11 molecular level^[22]. They are synthesized using sol-gel chemistry and are organized in five classes^[23]. The first
12 two classes of hybrids are both prepared by adding a polymer to a sol-gel synthesis. Class I is characterized by
13 weak O/I intermolecular interactions (molecular entanglement, hydrogen bonding and/or van der Waals forces),
14 while class II presents O/I covalent bonds. Class III and IV are hybrids characterized by the simultaneous
15 polymerization (one-pot synthesis) of both the organic and inorganic components. If O/I interactions are weak is
16 class III, if the organic and inorganic chains are covalently bonded is class IV. Finally, class V are a variation of
17 class III with a single silicate precursor able to liberate organic monomers that can then polymerize.

18 Our findings confirmed that class I PCL/BG hybrids have a strong osteostimulative potential in vitro, showing
19 strongly enhanced apatite formation, promotion of cell proliferation and of osteoblastic differentiation^[20]. These
20 results were corroborated in vivo in a mouse calvaria model, where tissue ingrowth was significantly increased
21 compared to a commercial benchmark^[21]. Sol-gel silicates were also found to be particularly effective in the
22 incorporation of antibiotics and their subsequent controlled release, thanks to templating effects occurring
23 during synthesis^[24]. In light of these promising findings, the aim of this work was to engineer a material with the
24 beneficial properties of PCL-based hybrids in terms of bone regeneration and simultaneous antibacterial effect:
25 a platform technology with a dual and decoupled controlled release of therapeutic silicates and an osteomyelitis-
26 specific antibiotic, rifampicin. Rifampicin is an RNA synthesis blocker very effective in the treatment of
27 staphylococcal infections, especially when delivered locally^[7]. PCL/silica hybrids were chosen as candidate for
28 the design and development of antibiotic bone fillers with superior performance both in term of long-term
29 controlled release of the drug and regenerative potential when compared to current competitors (e.g., PMMA,
30 CSC). To reach the purpose, the hybrid synthesis protocol was adapted to allow the incorporation of rifampicin
31 without significant degradation of the antibiotic. Preliminary dilution assays were performed to identify the
32 cytocompatibility concentration range and minimal inhibitory concentration of the antibiotic for the tested
33 bacterial strains. In parallel, an array of rifampicin-loaded PCL/silica hybrids with several drug loadings was
34 successfully prepared and physicochemically characterized. In particular, the release of therapeutic agents from
35 the materials, namely silicates and rifampicin, was measured to match the desired beneficial concentrations of
36 both. Finally, a biological characterization was carried out in order to confirm the efficacy of the hybrids in
37 terms of osteostimulation (on rat primary osteoblasts) and antibacterial effect (against *Staphylococcus aureus*,
38 *Escherichia coli* and *Pseudomonas aeruginosa*).

39

1 **2 Experimental section**

2 **2.1 Identification of a rifampicin concentration range of interest**

3 *2.1.1 Rifampicin minimum inhibitory concentration*

4 A set of preliminary dilution assays was initially performed in order to determine the minimum inhibitory
5 concentration (MIC) of rifampicin and identify the region of interest of concentration for this study. Three
6 relevant bacterial strains were considered: *Staphylococcus aureus* (clinical isolate from osteoarticular infection,
7 previously fully characterized elsewhere^[25–27]), *Pseudomonas aeruginosa* (ATC 27853) and *Escherichia coli*
8 (ATCC 25922). Isolated colonies of each strain were cultured overnight in nutrient broth (LB broth Lennox,
9 CONDA) at 37 °C under agitation (100 rpm), resulting in bacteria suspensions of $\sim 10^9$ CFU/mL the following
10 day. The suspensions were diluted to 10^6 CFU/mL by adjusting their optical density at 600 nm (Genesys™ 30
11 spectrophotometer, Thermo Fisher Scientific). The final inoculum was mixed with an array of subsequent
12 dilutions of rifampicin in alpha Minimum Essential Medium (α MEM, Gibco) ranging from 0 to 200 μ g/mL. At
13 four concentrations (0, 1, 10 and 50 μ g/mL), a standard Gram staining (gentian violet/fuchsin) was also
14 performed to characterize the strains and observe possible changes in cell shape following the exposure to
15 rifampicin.

16 *2.1.2 Rifampicin cytocompatibility range*

17 Rat primary osteoblasts (RPOs) were isolated from the enzymatic digestion of fetal Wistar rat calvaria explants
18 following a previously described method^[28]. In short, bone pieces were incubated for 15 minutes in a solution of
19 penicillin/streptomycin (p/s, 1%), collagenase IA (0.1%), and dispase II (0.2%) in cell culture α MEM. The
20 process was carried out at 37 °C and repeated four times. The obtained RPOs were then plated at 10,000
21 cells/cm² and cultured (37°C, 90% humidity and 5% CO₂) in α MEM supplemented with 10% fetal bovine serum
22 (FBS) and 1% p/s until confluence. Finally, the cells were collected and frozen in α MEM with 20% FBS and
23 7% dimethyl sulfoxide (DMSO) until the time of testing. To obtain a first set of information regarding the
24 interaction between rifampicin and RPOs the cells were cultured in presence of the antibiotic. RPOs were
25 seeded in 24-well plates at a density of 20,000 cells/well (as per supplier guidelines) and cultured for one week
26 using α MEM with 10% FBS, 1% p/s and various concentrations of rifampicin ranging from 0 to 100 μ g/mL. At
27 two time points (2 and 7 days) the cell viability was measured using XTT Viability/Proliferation Kit II (Sigma-
28 Aldrich), a colorimetric tetrazolium-based assay that correlates the viability of cells with the absorbance at 550
29 nm. The test was performed according to the protocol provided by the supplier.

30 **2.2 Synthesis of PCL/silica hybrids with and without rifampicin**

31 Polycaprolactone/silica hybrids with a 70:30 organic-to-inorganic ratio were synthesized by sol-gel chemistry
32 from tetraethyl orthosilicate (TEOS) (99% purity, Sigma-Aldrich). TEOS was initially dispersed in absolute
33 ethanol (Sigma-Aldrich) and hydrolyzed for 30 minutes adding 2 M HCl (diluted from 37% fuming HCl,
34 Sigma-Aldrich). The molar ratio between the components was ethanol : H₂O : TEOS : HCl = 3.7 : 2 : 1 : 0.07,
35 according to a previously optimized protocol^[20]. In parallel, polycaprolactone (PCL, Mn = 80 kDa, Sigma-
36 Aldrich) was dissolved in tetrahydrofuran (THF) at a concentration of 20% w/v. Once the polymer is completely
37 dissolved, rifampicin ($\geq 97\%$, suitable for cell culture, Sigma-Aldrich) can be incorporated into the hybrid: three
38 different quantities of antibiotic (see Table 1) were first dissolved into a negligible volume of solvent and then
39 added to the PCL solution. Control samples (PS) were synthesized omitting this step.

Table 1: Summary of the organic/inorganic (O/I) ratio and the rifampicin content of the four formulations of hybrid synthesized in this study

Formulation Name	Rifampicin content per gram of material (mg)	Theoretical PCL:SIO ₂ :rifampicin weight ratio
PS	0	70 : 30 : 0
PSRL	0.36	69.993 : 30 : 0.007
PSRM	3.6	69.93 : 30 : 0.07
PSRH	18	69.7 : 30 : 0.3

After the hydrolysis of TEOS, a saturated solution of NaOH (Sigma-Aldrich) in ethanol was prepared, filtered (0.2 μm PVDF syringe filter, Thermo Scientific) and added dropwise to the TEOS solution until the pH, initially very low (i.e. < 0), is adjusted to 5. This increase allows for the condensation of the silicate precursor in the sol, ultimately leading to its gelation, while also protecting the antibiotic from degradation. Right before complete gelation, the PCL and TEOS solutions are mechanically mixed and sonicated for 1 hour to obtain a homogeneous hybrid sol. The sol is aged for 24 hours before letting the solvent evaporate, obtaining hybrid films. The films were grinded and compressed into standard 100 mg pellets ($\varnothing = 13$ mm) used in all characterizations.

2.3 Physicochemical characterization

2.3.1 Stability in simulated physiological conditions

The stability of hybrids in a biological environment was tested in vitro by monitoring weight loss and pH variation over a period of 14 days in αMEM . Samples ($n = 5$) were immersed in the medium and incubated at 37°C for two weeks. The medium was refreshed every two days. Both pH and sample weight were measured at several time points (1, 3, 7 hours and 1, 3, 5, 7, 10, 14 days).

2.3.2 Contact angle

The surface wettability of PCL/silica hybrids with and without rifampicin was also investigated to identify possible variations in hydrophilicity following the addition of the antibiotic. Static contact angle measurements were performed at room temperature using a simple custom set-up consisting of a manually adjustable base and a microliter syringe (25 μL Model 702 N, Cemented Needle, 22s gauge, 2 in, point style 2, Hamilton Company). A 10 μL droplet was initially deposited on the sample. Then, after a one-minute lag to reduce the impact of absorption on the results, images of the contact angle were acquired using an industrial camera UI-3370CP Rev.2 (4 MP CMOS sensor CMV4000) equipped with a Sigma 105 mm f/2.8 macro lens (Imaging Development Systems, IDS). Three independent measurements per sample type were performed, with two angles (left and right) per measurement. Contact angle calculation was carried out using ImageJ (NIH, USA) with prior image elaboration on GIMP (thresholding, brightness/contrast correction, color inversion).

2.3.3 Fourier-transform infrared spectroscopy

Fourier-transform infrared spectroscopy (FTIR) was used to characterize the chemical nature of the materials. The acquisition of infrared spectra of all samples was carried out using a Nicolet 380 FT-IR (Thermo Fisher Scientific) equipped with a diamond Attenuated Total Reflectance (ATR) accessory. Data (32 scans, resolution of 4 cm^{-1}) were collected in the mid-IR region (4000–400 cm^{-1}) in triplicates and from different regions of each sample.

1

2 **2.4 Controlled release of ions and antibiotic**

3 *2.4.1 Extraction of loaded rifampicin*

4 To estimate the efficacy of our synthesis route, a protocol of extraction and quantification of the rifampicin
5 loaded in the hybrids was developed. The results were compared to the theoretical drug concentration per
6 formulation (as per Table 1). To retrieve the antibiotic loaded into the materials, 100 mg of all hybrid
7 formulations were left to dissolve in 10 mL of THF for 2 days. Two cycles of sonication were also performed, at
8 24 and 48 hours, respectively. This results in the formation of a suspension of inorganic silicate nanoparticles
9 (insoluble in the solvent) dispersed in a PCL and rifampicin solution in THF. The suspensions were centrifuged
10 for 1 minute at 2000g, then the supernatant was collected and stored for further analysis.

11 *2.4.2 Rifampicin release*

12 The release of antibiotic was characterized in colorless α MEM. The lack of phenol red (pH indicator) avoids
13 possible alterations of the spectra. Rifampicin-loaded hybrids were immersed in the medium and incubated in an
14 orbital shaker at 37°C and 250 rpm. At selected time-points (1, 3, 5, 7, 10 and 14 days) the medium was
15 retrieved and tested to quantify its concentration in antibiotic.

16 *2.4.3 First derivative UV-Vis spectrophotometry*

17 A spectrophotometric method developed by Walsh *et al.*^[29] was used to quantify rifampicin in both the
18 solutions retrieved from hybrids (loading efficacy) and in released products in α MEM. At every experiment, a
19 calibration curve was prepared using known concentrations of rifampicin in a relevant solvent (α MEM or THF,
20 depending on the experiment). According to the method, the amount of rifampicin is proportional to the value of
21 the first derivative of the absorbance at 500 nm.

22 *2.4.3 Quantification of silicon release by ICP-OES*

23 The release of silicon ions (in the form of various silicates, such as silicic acid) was performed in α MEM and
24 measured by Inductively Coupled Plasma Optical Emission Spectrometry (ICP-OES). Standard hybrid pellets of
25 all formulations were immersed in culture medium at a 20 mg/mL ratio and put in an orbital shaker at 37°C and
26 250 rpm. At given time-points the medium was retrieved and the concentration of Si ions was determined by
27 ICP-OES (Ultima C, HORIBA Jobin Yvon). It is known from previous studies that the release profile of this
28 type of hybrids is relatively steep (i.e., it reaches plateau within the first few days). Therefore, the chosen time-
29 points were 30 minutes, 1, 3, 5, 7 hours and 1, 2, 3 days.

30 **2.6 Microbiology**

31 *2.6.1 Agar disk diffusion test*

32 A first estimation of the antibacterial properties of rifampicin-loaded hybrids was obtained by an agar disk
33 diffusion assay (halo test). Bacteria populations of *S. aureus* (clinical isolate), *P. aeruginosa* (ATC 27853) and
34 *E. Coli* (ATCC 25922) in LB broth were prepared as described in section 2.1.2 and then diluted down to a
35 density of circa 10^7 CFU/mL. This value is high enough to grant the development of an even layer of colonies
36 on the agar plate. The adjusted inoculum was deposited and spread homogeneously onto a petri dish ($\varnothing = 94$
37 mm) filled with Agar LB Miller (CONDA). A sample per formulation was then set on top of the agar and the

1 dish was incubated for 24 h at 37°C and high relative humidity (80%). The width of the inhibition annulus was
2 then calculated as the difference between external radius and internal radius (i.e., 7.5 mm).

3 4 *2.6.3 Colony forming units counting and antifouling test*

5 Quantitative evaluation of the antibacterial effect of rifampicin-loaded hybrids was also carried out by colony
6 forming units (CFUs) counting using the same strains as above. Suspensions of the three bacteria in α MEM
7 (density = 10^6 CFU/mL) were incubated for 24 hours in presence of pellets of all the synthesized formulations.
8 The same medium used for eukaryotic cells was chosen for better comparison between the results of
9 microbiology and the ones obtained when studying RPOs. At given time-points (3, 6 and 24 hours) each
10 suspension was retrieved, diluted according to need and plated LB on agar petri dishes using an automatic
11 diluter and plater (easySpiral Dilute, Interscience). In parallel, the number of bacteria adhering on the pellets
12 was also measured to estimate possible antifouling properties of the materials. Pellets were rinsed three times in
13 saline (ϕ), then immersed in 5 mL of ϕ and sonicated for 10 minutes to detach cells from the surface.
14 Afterwards pellets were disposed of and the remaining bacterial suspension in ϕ was diluted when necessary and
15 plated on agar. After further 24 hours of incubation, colonies were counted using an automatic colony counter
16 (Scan 300, Interscience).

17 **2.7 Osteoblast response**

18 *2.7.1 Cytotoxicity and cell viability*

19 RPOs were cultured in presence of the dissolution products of antibiotic-loaded hybrids to evaluate possible
20 cytotoxicity and characterize their influence on cell viability and proliferation. RPOs were seeded at a density of
21 20,000 cells per well and cultured for one week using eluates of the materials in α MEM (with 10% FBS and 1%
22 p/s). As described in section 2.1.1, cell viability was assessed at 2 and 7 days using the XTT
23 Viability/Proliferation Kit II (Sigma-Aldrich), which correlates viability with the respective value of absorbance
24 at 550 nm.

25 *2.7.2 Cell adhesion and morphology*

26 Cells were also cultured directly on the hybrid samples in order to observe cell morphology and investigate
27 possible changes in adhesion. RPOs were seeded on the surface of PSRM pellets and cultured in α MEM
28 overnight. On the second day, the samples were fixed using 1.6% glutaraldehyde in 0.2M sodium cacodylate
29 buffer (pH 7.4). They were stored in the fixative for 4 days at 4°C. Subsequently, they were washed three times
30 with a sodium cacodylate buffer and post-fixed 1 hour with 1% osmium tetroxide. After an additional wash in
31 distilled water, samples were dehydrated by graded ethanol, treated with hexamethyldisilazane (HMDS) and
32 dried overnight. Scanning electron microscopy (SEM) was performed upon sputter coating with carbon
33 (Emitech E6500, Quorum) using a Regulus 8230 (Hitachi) at 2kV.

34 *2.7.3 ALP activity*

35 A preliminary investigation of the osteostimulative effect of silicates release from the hybrids was performed by
36 measuring variations in the activity of enzymatic alkaline phosphatase (ALP) at 14 days of culture. RPOs were
37 cultured as described in previous sections. At the desired time-point, culture wells were washed three times in
38 PBS and treated with NP40 lysis buffer. Resulting cell lysates were incubated in a solution of 40 mM p-
39 nitrophenyl phosphate (Sigma-Aldrich) and alkaline assay buffer (Abcam). The production of p-nitrophenol as a

1 function of the ALP activity was determined by spectrophotometric measurement at 405 nm and at 37 °C. The
2 absorbance was expressed as the mean value per minutes. Results were normalized with respect to the total
3 amount of proteins in the respective sample as obtained by a bicinchoninic acid (BCA) assay.

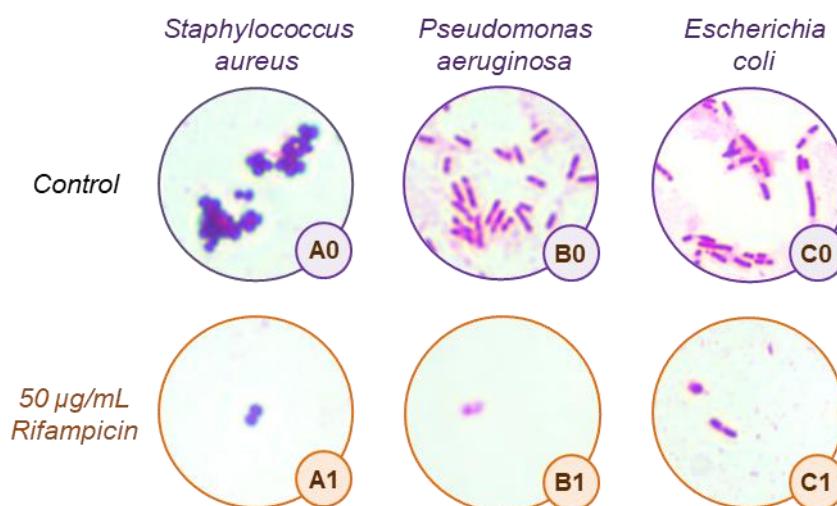
5 2.8 Statistical analysis

6 Results of each population were given as the mean \pm standard deviation (SD). Comparisons to highlight
7 statistically significant differences were performed by one-way analysis of variance (ANOVA) with a
8 significance of $\alpha = 0.05$ (OriginLab 8.5 data analysis software).

9 3 Results and discussion

10 3.1 Rifampicin tailoring

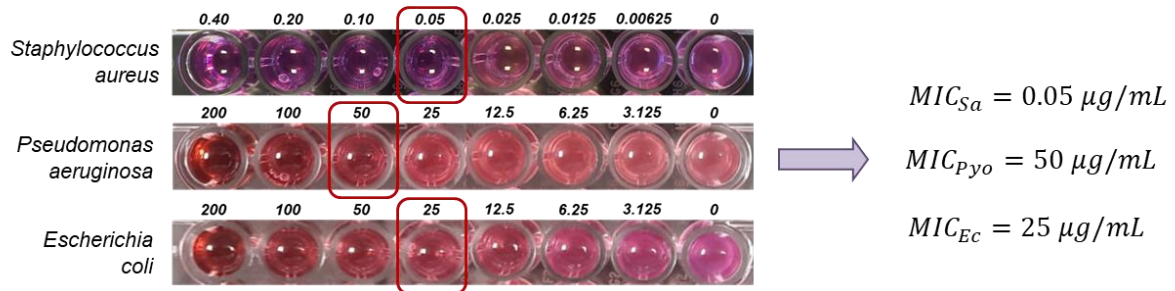
11 Prior to material preparation, the effect of rifampicin on the target cells, both eukaryotic and prokaryotic, was
12 characterized. This step supports the design of the controlled release platform, providing valuable information
13 on the effective concentration ranges to inhibit bacteria without exerting major detrimental effects on
14 osteoblasts. Observations after Gram staining indicated that samples exposed to rifampicin show a significantly
15 lower number of bacteria, often tending to zero. An interesting morphological phenomenon associated with high
16 concentrations of rifampicin was also assessed with the two Gram negative bacilli: cells appear smaller and with
17 a round shape (Figure 1, panels B1 and C1). Rifampicin is known to significantly alter the attachment points of
18 the nucleoid to the cell membrane in *E. coli*^[30]. However, to date we found no information on possible effects of
19 the drug on the overall cell morphology and these changes are likely due to a global reaction to the stress
20 induced by the antibiotic. In addition, no such variation was detected for *S. aureus*, possibly as a consequence of
21 its higher susceptibility to rifampicin, which impedes the onset of reactive mechanisms by the cells.



22
23 **Figure 1:** Gram staining of the three bacteria used in this study cultured in standard conditions (top, A0 to C0)
24 and in presence of a rifampicin concentration of 50 µg/mL (bottom, A1 to C1).

25 Levels of MIC can vary according to strains^[31], bacterial genomic variations (i.e., resistance development)^[32]
26 and culture and testing conditions^[33]. These variations can often be significant, up to three or four orders of
27 magnitude. In this study, the dilution assays performed with the three bacterial strains of interest in the context

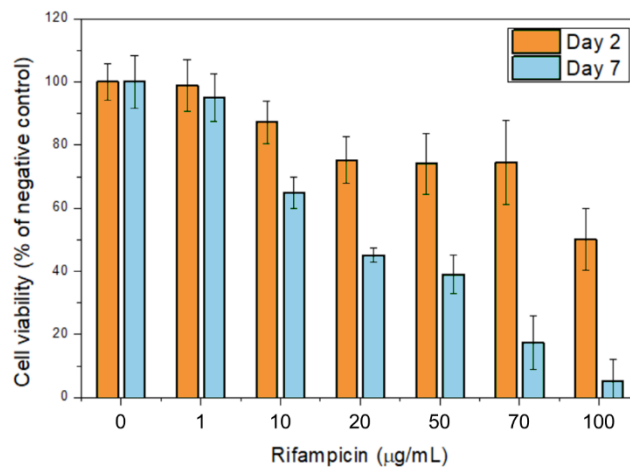
1 of osteomyelitis allowed the determination of the MIC of rifampicin against *S. aureus*, *P. aeruginosa* and *E. coli*
 2 at 0.05 µg/mL, 50 µg/mL and 25 µg/mL, respectively (Figure 2).



3
 4 **Figure 2:** Rifampicin dilution arrays used to identify the MICs of the strains *S. aureus* (Sa), *P. aeruginosa* (Pyo)
 5 and *E. coli* (Ec). Each MIC corresponds to the lowest concentration leading to a clear (i.e., not turbid)
 6 suspension. The values are highlighted and reported on the right.

7 Regardless of the strain, MIC values measured in this study were generally consistent with current results found
 8 in literature. The clinical strain of *S. aureus* tested in this study was found to be highly susceptible to rifampicin.
 9 Relatively higher values were obtained with the two Gram-negative strains. This is not surprising, since these
 10 bacilli are generally known for their lower susceptibility to the molecule^[34].

11 A similar approach was adopted for the determination of RPOs cell behavior in presence of rifampicin. Cell
 12 viability was measured using XTT at 2 and 7 days of incubation. The results of the test are reported in Figure 3.



13
 14 **Figure 3:** Cell viability of rat primary osteoblasts (RPOs) at 2 and 7 days as a function of rifampicin
 15 concentration (0 – 100 µg/mL). Data at each day are normalized with respect to the viability of the respective
 16 negative control. The progressive inhibition of RPOs and the cytotoxic effect at higher concentrations (> 10
 17 µg/mL) can be clearly observed.

18 A decrease in viability can be observed already at 2 days, starting above 10 µg/mL and increasing dose-
 19 dependently. Up to 70 µg/mL, the reduction is limited, with viability sitting around 70-80% of the control.
 20 However, 100 µg/mL of rifampicin were found to halve the viability already at 2 days. The results were
 21 confirmed by examining the viability RPOs after one week of culture: a significant decrease to 70% of the
 22 control was measured already for cells exposed to 10 µg/mL of rifampicin. At 50 µg/mL the values are as low as
 23 40%, decreasing to almost no viability at 100 µg/mL. Similar results were obtained by Winters *et al.*^[35], who
 24 confirmed the absence of specific cytotoxic effects of rifampicin on human cells up to 20 µg/mL. Differently,

1 studies of the effect of rifampicin showed no cytotoxic effect up to 85 $\mu\text{g}/\text{mL}$ when using a hepatic cell line
 2 (HepG2)^[36]. Probably due to the more sensitive nature of primary cells compared to cell lines, our data suggest
 3 that high concentrations of rifampicin have a significant cytotoxic effect. For this reason, in view of the design
 4 of the hybrid materials, the release concentration was tailored in the 0 to 20 $\mu\text{g}/\text{mL}$ range.

5 3.2 Sol-gel synthesis, rifampicin loading efficacy and in vitro degradation behavior

6 Homogeneous PCL/Silica hybrids with and without rifampicin were successfully synthesized. In particular, the
 7 process appears reproducible, resulting in materials with antibiotic evenly distributed within the network.
 8 Burning out the organic component of the hybrids at high temperature also confirmed that the organic-to-
 9 inorganic ratio is in accordance with its theoretical value of 70:30, only slightly lower (Table 2). The difference
 10 is probably due to a partial burn-out of low molecular weight inorganic residues.

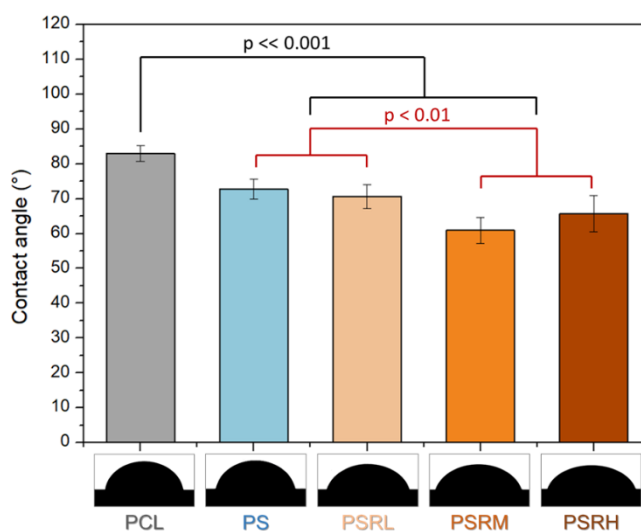
11 **Table 2:** Summary of the weight percentages of the inorganic component (theoretical value = 30%), the
 12 theoretical loaded rifampicin and the measured antibiotic retrieved from the materials after synthesis (both
 13 expressed as mass per 100 mg sample).

Formulation name	Inorganic fraction (%)	Theoretical loaded rifampicin per sample (μg)	Measured loaded rifampicin per sample (μg)
PS	27.6 ± 1.3	0	1 ± 2
PSRL	26.5 ± 2.1	36	32 ± 15
PSRM	27.1 ± 1.6	360	280 ± 60
PSRH	25.8 ± 1.9	1800	1800 ± 100

14
 15 Although a key topic surrounding the synthesis of organic/inorganic hybrids is the incorporation of calcium ions
 16 for increased apatite forming ability^[22,37], in this study materials with pure silica as inorganic component were
 17 prepared. In early trials (data not shown), we observed the occurrence of a very rapid and significant
 18 degradation of rifampicin in presence of either high pH or calcium ions. This characteristic of the drug makes it
 19 incompatible with previously adopted synthesis protocols used for the preparation of binary Si-Ca hybrids.
 20 Therefore, in this study calcium was removed and a minimum amount of sodium was used to adjust the pH of
 21 the solution pot to a value that maximizes rifampicin stability (i.e., pH ~ 5). The spectrophotometric results on
 22 loading efficacy confirmed that this technique did not significantly degrade rifampicin. The right columns of
 23 Table 2 show the measured and theoretical content of rifampicin loaded in each pellet sample (100 mg)
 24 depending on the hybrid formulation. Little to no variation between the two values was observed for every
 25 tested material. Note that for PSRL the standard deviation is relatively high since the amount of rifampicin
 26 loaded is minimal and rather close to the sensitivity threshold of spectrophotometry. Since the selected
 27 spectrophotometric method is specific for rifampicin and not its degradation products^[29], it is safe to assume that
 28 loading PCL/silica hybrids with rifampicin does not significantly hinders the structure (and thus the antibacterial
 29 effect) of the antibiotic.

30 A statistically significant, although minor, effect of rifampicin was observed when studying the wettability of
 31 the samples. Contact angle measurements identified two distinct phenomena: (i) an increase in hydrophilicity in
 32 PCL/silica hybrids compared to a PCL control and (ii) a less prominent, but nevertheless significant, decrease in
 33 contact angle following rifampicin loading. In general, contact angles measurements were in line with values

1 reported in literature for similar materials, both for PCL^[38,39] and its hybrids^[20]. PCL showed a rather typical
 2 mild hydrophobic behavior ($\theta = 83^\circ \pm 2$), reduced after the addition of silica. The incorporation of the inorganic
 3 component determines a statistically significant increase in hydrophilicity, expressed as a decrease of circa 10°
 4 in contact angle. This increase can be beneficial to cell adhesion^[40]. While PSRL is comparable with PS, a
 5 further decrease of 5-10° compared to the PS control was observed for higher loadings of rifampicin (PSRM and
 6 PSRH), indicating that the antibiotic contributes to the overall hydrophilicity of the material despite its modest
 7 amount (see Table 1). This is somewhat surprising since rifampicin is generally considered hydrophobic^[41].



8
 9 **Figure 4:** Droplet profiles and contact angle measurements for all formulations of PCL/silica tested (n = 3).
 10 Note the effect of both the introduction of silica gel (p << 0.001) and of rifampicin (p < 0.01) on the
 11 hydrophilicity of the samples.

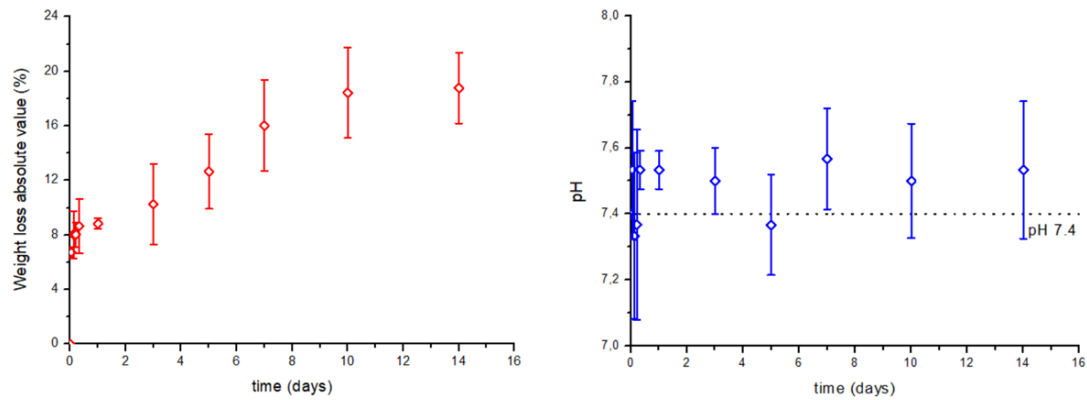
12 The stability of the hybrids in a suitable medium was then investigated. Rifampicin was found to have negligible
 13 effects on the degradation behavior of the materials. As confirmed by monitoring the weight variation in
 14 α MEM, no variation was observed following the addition of antibiotic. All samples followed a typical trend
 15 already reported for class I polycaprolactone-based hybrids by Bossard *et al.*^[20]: an initial loss of soluble
 16 inorganic moieties, followed by a higher decrease due to the de-esterification of PCL, reaching a weight loss of
 17 15-20% after 14 days (Figure 5). The degradation rate significantly differ from the reported value of 13.2%
 18 weight loss after 8 weeks^[20]. However, previous results were obtained in static conditions, while in the present
 19 study semi-dynamic conditions were preferred. It is possible that medium renewal accelerated the degradation of
 20 PCL^[42].

21 In parallel, possible changes in pH were also monitored. Data seem to suggest the occurrence of a minor
 22 increase in pH probably associated with the leaching of residues of sodium used during the synthesis. The
 23 increase was found to be not statistically significant, indicating that the hybrids do not hinder the buffer capacity
 24 of α MEM and thus do not create an alkaline and possibly harmful microenvironment for cells, as it is sometimes
 25 the case for bioactive glasses^[43].

26 Both weight loss and pH measurements confirmed that PCL/silica hybrids are stable in simulated physiological
 27 conditions, degrading slowly and evenly, and show low risk of cytotoxicity due to alkalinization of the medium.
 28 They can be deemed appropriate carriers for the long-term delivery of rifampicin. In addition, as already

1 suggested by other authors^[20,44], these hybrids offer superior degradation properties compared to other candidate
2 materials for bone grafting and orthopedic applications.

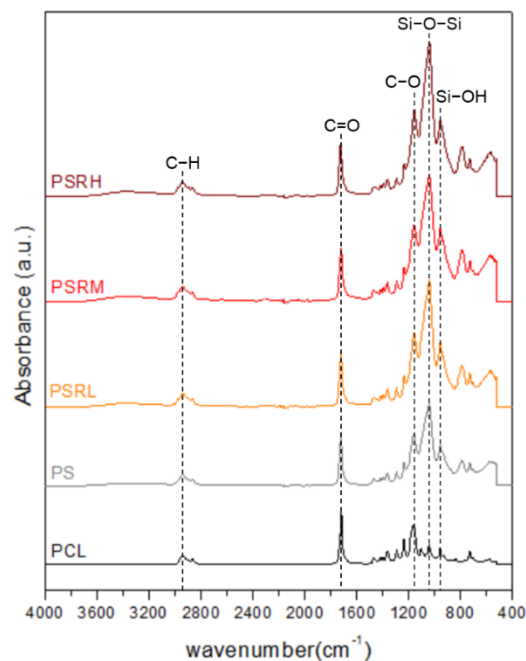
3



4

5 **Figure 5:** Graphs showing a typical trend for weight loss (left) and pH (right), following immersion in culture
6 medium for PCL/silica hybrids (results for PSRM are shown, other samples are comparable). The measurements
7 are not affected by the addition of rifampicin: no statistically significant variation was observed varying the
8 concentration of antibiotic ($p > 0.05$, see supplementary data).

9 The characterization with ATR-FTIR was used to study the chemical nature of the two phases, organic PCL and
10 inorganic silica, as well as on the interaction between them. In Figure 6 the FTIR spectra of PCL (as a control)
11 and all formulations are reported.

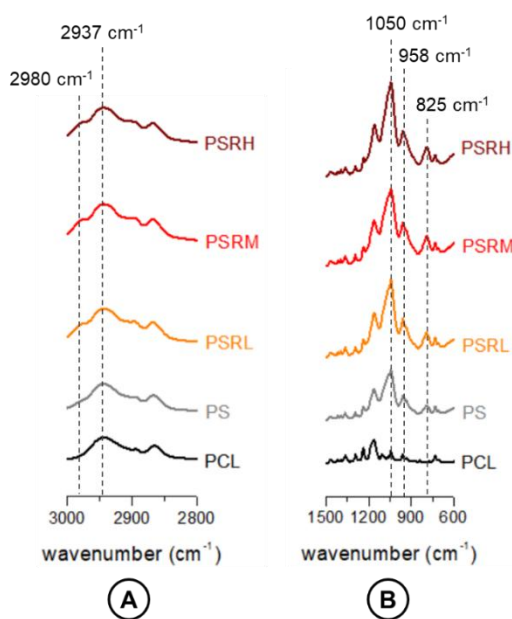


12

13 **Figure 6:** Comprehensive FTIR spectra ($4000-400\text{ cm}^{-1}$) of PCL (bottom) and the four formulations of
14 PCL/silica hybrids tested in our study. The major characteristic peaks of PCL (C-H, C=O, C-O), silica gel
15 (Si-O-Si, Si-OH) and rifampicin (C-H) are highlighted. All spectra are normalized with respect to the
16 characteristic peak of PCL at 1720 cm^{-1} .

1 Typical IR peaks of PCL were observed for all samples. In particular, two peaks of the asymmetrical and
2 symmetrical stretching of carbon-hydrogen bonds centered at 2937 and 2860 cm^{-1} ($\nu\text{C-H}$), the sharp
3 characteristic peak of PCL due to carbonyl stretching at 1720 cm^{-1} ($\nu\text{C=O}$), the peaks of carbon-hydrogen
4 bending between 1471 and 1365 cm^{-1} ($\delta\text{C-H}$) and the three peaks of the carbon-oxygen stretching of the ester
5 groups ($\nu\text{C-O}$) at 1294, 1240, and 1170 cm^{-1} . Once silica is introduced into the polymeric matrix, all the peaks
6 typically related to the vibrations of the Si-O-Si cage occur^[45]. Particularly evident are the symmetric and
7 asymmetric stretching at 825 cm^{-1} and 1050 cm^{-1} (Figure 7A), as well as a low wavenumber bending vibration
8 peak at 600 cm^{-1} .

9 Interestingly, only minor peaks associated with silanol groups were detected, indicating that the great majority
10 of TEOS reacted during the sol-gel process. This result is unexpected as hybrid systems are usually
11 characterized by significant Si-OH peaks, especially by the hydroxyl vibration of self-associated silanols,
12 centered at 3400 cm^{-1} . In addition, silanols are reported to highly change the shape of the characteristic peak of
13 PCL at 1720 cm^{-1} as a consequence of the H-bonds between silanols and the carbonyl groups of PCL^[46]. In this
14 study, this peak remains unvaried, regardless of the formulation. These observations led to the conclusion that
15 the preparation of the hybrid sol did not hinder the polycondensation of TEOS, leading to few unreacted silanols
16 and, as a consequence, to little H-bonding between the inorganic and organic component. The interaction
17 between the two components of a hybrid is known to be a major drive for the development of materials with
18 unique properties^[47]. For this reason, improving the organic-inorganic interactions in antibiotic-loaded
19 PCL/silica hybrids could offer promising future developments.



20

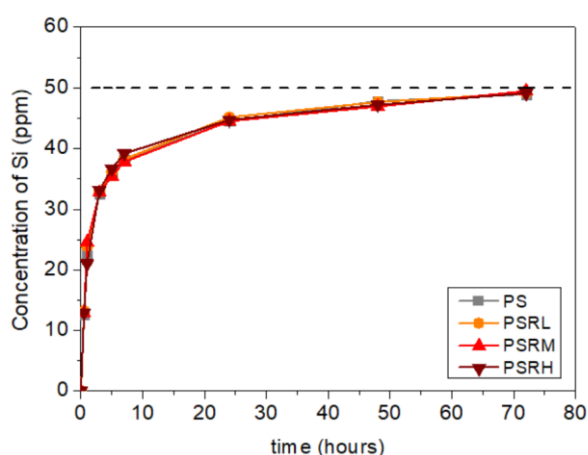
21 **Figure 7:** (A) FTIR spectra highlighting the appearance of a new peak at 2980 cm^{-1} in correspondence of the
22 stretching vibration of C-H following the addition of rifampicin. (B) FTIR spectra comparing the 1500-900 cm^{-1}
23 range before and after sol-gel synthesis. Note the carbon-oxygen ester stretching of PCL at 1170 cm^{-1} and the
24 appearance of peaks associated with silica gel: Si-O-Si (1050 and 825 cm^{-1}) and Si-OH (958 cm^{-1}).

25 The FTIR analysis was also used in order to confirm the presence of rifampicin in the samples. Unfortunately,
26 when adding rifampicin, only minor variations were observed. This was probably due to (i) the low amount of

1 antibiotic compared to the overall mass of the material and to (ii) the overlapping between the characteristic
2 peaks of rifampicin and PCL, especially in the 1000-1500 cm^{-1} range. However, two small differences were
3 observed following antibiotic loading: the occurrence of a new shoulder peak at 2980 cm^{-1} and a significant
4 increase in intensity of the peak at 958 cm^{-1} (Figure 7B). These variations are consistent with the occurrence of
5 interactions between rifampicin and its carrier matrix^[16]. An alternative hypothesis is that the 958 cm^{-1} can be
6 ascribed to minor Si-OH stretching while the shoulder peak to the vibrations of methyl and methylene groups in
7 rifampicin^[48]. These results substantiate the successful loading of rifampicin, as previously verified by
8 spectrophotometry. However, due to the weakness of the signal, the results in this respect cannot be deemed
9 conclusive. Therefore, infrared spectroscopy should be avoided when investigating the rifampicin content in
10 PCL/silica hybrids.

11 3.3 Dual and decoupled release of therapeutic agents

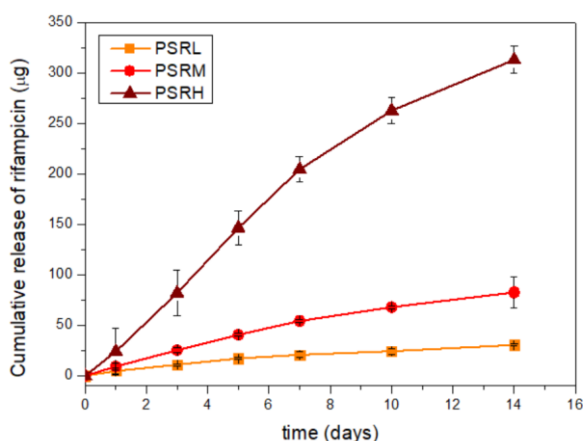
12 Rifampicin-loaded PCL/silica hybrids are characterized by the ability of releasing therapeutic agents with
13 potential beneficial effects on the proliferation of osteoblasts and the inhibition of bacterial growth. Before
14 testing the biological performance of the materials, the release of therapeutics was evaluated immersing samples
15 in α MEM. Silicate release from the inorganic component of the hybrids was measured by ICP-OES (Figure 8).
16 Results indicate that the concentration of Si ions in the medium quickly increase, reaching a plateau of
17 saturation of circa 50 ppm after the first day of immersion. As expected, no variation associated with rifampicin
18 loading was observed, given that the organic-to-inorganic ratio remained unvaried across all formulations. The
19 rapid silicon burst release in simulated body fluids is a well-documented phenomenon for similar hybrid
20 materials^[20,21] and silica-based sol-gel glasses^[49,50]. If medium is replenished, the burst repeats with similar
21 kinetics, presenting a steady concentration silicates in the aqueous environment, up to the solubility limit of
22 silica in water (~ 50 ppm). These silicates are known to have osteogenic effects on eukaryotic cells, including
23 promotion of osteoblastic differentiation, bone mineralization and secretion of extracellular matrix (ECM)^[51].
24 Our results corroborate the hypothesis that PCL/silica hybrids could offer a beneficial sustained release of
25 silicates supporting cells during the first phases of adhesion and differentiation.



26
27 **Figure 8:** Silicon release from PCL/silica hybrids immersed in α MEM. As expected, concentrations measured
28 by ICP-OES do not vary depending on the rifampicin content.

1 The release of rifampicin was measured calculating the first derivative of the absorbance at 550 nm, which was
2 previously confirmed to be specific for the quantification of the antibiotic^[29]. Direct UV-Vis determination of
3 rifampicin can also be performed by measuring the peaks at 330 and 475 nm. However, the derivative technique
4 is more robust and accurate. In particular, it can detect the drug even in presence of its degradation products
5 (mainly 3-formyl rifampin and rifampin quinone), expected to be present as a consequence of sol-gel synthesis.
6 The spectrophotometric results showed that a remarkable almost linear trend of release over 14 days of
7 immersion in medium (Figure 9). This confirms that PCL/silica hybrids can be considered as an ideal candidate
8 when it comes to delivering a sufficient quantity of rifampicin over a long period of time without possibly
9 harmful burst release. This property could effectively protect from infections even several weeks after
10 implantation. For instance, after 14 days of immersion, 30.7 μg , 82.8 μg and 313.5 μg of rifampicin were
11 released by PSRL, PSRM and PSRH, respectively. These quantities account for the 85%, 23% and 17% of the
12 total antibiotic loaded in each formulation. The quantification shows that the released amount of rifampicin
13 depends on the quantity initially added to the materials, confirming that the delivery of antibiotic can be
14 controlled by tailoring its loading.

15 The performance of our candidates was also satisfactory when compared to previously reported approaches for
16 the local delivery of rifampicin. Polymer-based technologies are generally characterized by a rapid burst. For
17 instance, drug release was reported to reach 100% within the first day using either polyhydroxybutyrate
18 microsphere^[52] or chitosan gels^[53]. Better results could be obtained using inorganic strategies, probably thanks
19 to the interaction between the inorganic matrix and the drug^[16]. For instance, investigations into a biphasic bone
20 cement material composed of calcium sulphate (CaSO_4) and nano-hydroxyapatite reported a similar sustained
21 release trend, slowly ramping to 25-30% of released rifampicin after 2 weeks of immersion^[16]. The use of
22 hybrids as carriers could offer an additional improvement over CaSO_4 -based cements owing to their superior
23 mechanical and degradative properties^[54]. In addition, class I PCL hybrids already have a promising history of
24 *in vivo* regeneration potential compared to more inert candidates currently in use^[21].



25
26 **Figure 9:** Cumulative release of rifampicin from all the formulations of tested samples. The antibiotic content in
27 the medium is dependent on the loaded amount, confirming that this technology can be used to tailor rifampicin
28 release.

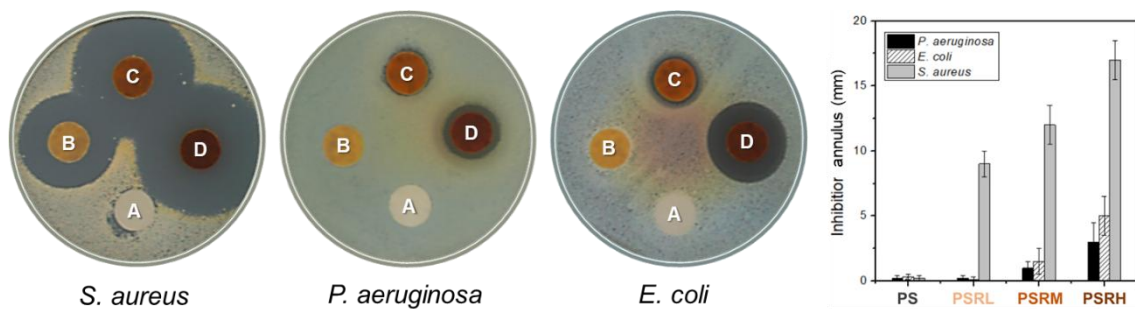
29 When it comes to surgical site infections, the initial stages after implantation are often the most critical. The
30 release after 24 hours should be assessed to gain more insight into the potential of the materials. PSRL, PSRM

1 and PSRH delivered 4.9 µg, 9.3 µg and 24,1 µg of antibiotic, respectively. These quantities correspond to
2 concentrations of 0.98 µg/mL, 1.86 µg/mL and 4.82 µg/mL, all significantly above the MIC of rifampicin for *S.*
3 *aureus* (0.05 µg/mL). However, they are lower than the MICs of *E. coli* and *P. aeruginosa* (25 µg/mL and 50
4 µg/mL), indicating that the technology against these two strains might not be effective. To gain more insight
5 into the matter, an in-depth investigation of the antibacterial properties of the three formulations of rifampicin-
6 loaded PCL/silica hybrids was performed.

7 3.4 The release of antibiotic is highly effective against common osteomyelitis strains

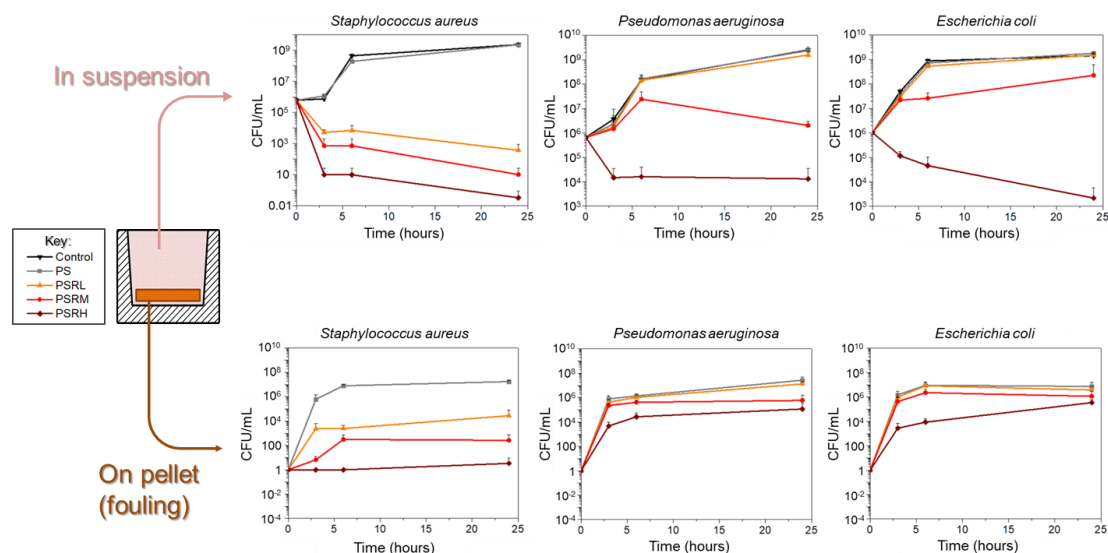
8 The antibacterial analysis of the materials was carried out in two subsequent steps. First, a preliminary agar disk
9 diffusion assay was used to gain preliminary data on potential of each formulation. Then, CFU counting was
10 performed in order to quantify the bactericidal effect.

11 The results of the halo test reflect the findings of the dilution assays used to determine the MICs for the tested
12 strains. Rifampicin was successfully released from all loaded hybrids with dose-dependent inhibition zones
13 significantly increasing with higher rifampicin loading ($p < 0.05$). As expected from the MIC determination,
14 inhibition areas were wider for *S. aureus* and smaller for both the tested Gram-negative strains. No halo was
15 observed for pure PCL/silica samples, confirming the lack of intrinsic antibacterial properties of the material.
16 Against *S. aureus*, rifampicin was already effective at the lowest dosage (PSRL), resulting in an inhibition zone
17 with a width of 9 mm. For PSRM and PSRH samples the width significantly increased to 12 and 17 mm,
18 respectively. Less remarkable was the effect against the two Gram-negative strains, as it is often the case with
19 this family of bacteria, known for their lower susceptibility to antibiotics and other antimicrobial agents owing
20 to their more complex and resistant cell wall structure. Despite this, the highest dosage of rifampicin (PSRH)
21 was proven effective against both *E. coli* (3 mm) and *P. aeruginosa* (5 mm width) without significant difference
22 between the two results. No inhibitory effect was found around PSRL. A minor inhibition zone (~ 1 mm width)
23 was instead observed around PSRM samples. This value is often indicated as the minimum threshold to validate
24 the inhibitory effect of an antibacterial material (SNV 195920-1992)^[55,56]. In light of this result, it can be
25 concluded that, while all formulations showed outstanding performance against *S. aureus*, the loading
26 concentration of rifampicin in PSRM can be considered as the lower limit of concentration for the design of
27 materials that target *E. coli* and *P. aeruginosa* and possibly other Gram-negative bacterial strains.



28
29 **Figure 10:** Images of a typical agar diffusion assay of PS (A), PSRL (B), PSRM (C) and PSRH (D) samples
30 against *Staphylococcus aureus*, *Pseudomonas aeruginosa* and *Escherichia coli*. On the graph on the right, a
31 quantification of the inhibition width is reported.

1 The results of CFU counting confirmed and expanded the preliminary findings obtained by the agar diffusion
 2 assay (Figure 11). In suspension, the results of the negative control were as expected, showing a growth curve
 3 typical of a healthy bacterial population: an initial lag phase in the first hours of culture, followed by exponential
 4 growth and finally by a plateau around 10^9 CFU/mL (10^7 on pellets)^[57]. Bacteria behaved similarly when
 5 cultured in contact with PS.



6
 7 **Figure 11:** Bacterial growth curves (CFU counting) for *S. aureus*, *P. aeruginosa* and *E. coli* in contact with all
 8 formulations of hybrids. Cells in suspension (top) and attached to the samples (bottom) were both counted.
 9 Empty culture wells with α MEM were used as negative control when relevant.

10 All rifampicin-containing formulations were highly effective against *S. aureus*, showing a remarkable reduction
 11 in bacterial growth between six (for PSRL) and nine (for PSRH) orders of magnitude. Against Gram-negative
 12 bacteria the reduction of the CFUs in suspension was less remarkable, but significant, nonetheless. In particular,
 13 PSRM inhibited the growth of *P. aeruginosa* and *E. coli* of a 3.0-log and 1.8-log, respectively. The inhibition
 14 then increases to more than 5-log when the two strains are put in contact with PSRH. The logarithmic reduction
 15 in bacterial growth for all formulations and strains is reported in Table 3. The antifouling properties of the
 16 materials were also tested by counting the number of bacterial cells that adhered to the pellets. Once again, the
 17 hybrids showed remarkable antifouling properties against *S. aureus*, significantly reducing the number of cells
 18 found on the samples in a dose-dependent fashion, from 2.8-log for PSRL to 6.7-log for PSRH. Bacterial growth
 19 on the pellets was also reduced in the case of *E. coli* and *P. aeruginosa*, although for these two strains the
 20 reduction was limited to 1-2 orders of magnitude and the bacteria were not susceptible to PSRL (see Figure 11
 21 and Table 3).

22 **Table 3:** Log₁₀ decrease of bacterial inhibition after 24 hours following the contact with rifampicin-loaded
 23 hybrids. The values are calculated with respect to the negative control (suspension) or to PS (pellet).

	PSRL		PSRM		PSRH	
	suspension	pellet	suspension	pellet	suspension	pellet
<i>S. aureus</i>	6.8	2.8	8.4	4.8	9.8	6.7
<i>P. aeruginosa</i>	0.2	0.3	3.0	1.7	5.2	2.4
<i>E. coli</i>	0.0	0.3	1.8	0.8	5.8	1.3

24

1 Results of the quantitative antibacterial testing confirmed the potential of rifampicin sustained release from
2 PCL/silica hybrids and helped clarify the optimal window of concentration to achieve a broader spectrum of
3 effect against both Gram-positive and -negative bacteria. According to our data, rifampicin loading equal and
4 superior to PSRM seems to give enough antibacterial effect to inhibit the growth of all tested strains tested. On
5 the other hand, PSRL is a good candidate against *S. aureus*, but did not show any effect against the Gram-
6 negative bacteria tested in this study. Considering the high density of the starting inoculum (i.e., 10^6 CFU/mL),
7 this experiment was designed as a worst-case scenario. In realistic settings, the entity of bacterial contamination
8 is several orders of magnitude smaller^[58] and the performance of PSRM against all strains can be considered
9 successful. In future work, increasing the loading of rifampicin towards the values of PSRH (e.g., double it)
10 might be a good strategy to improve the results. However, the content of rifampicin cannot be increased *ad*
11 *libitum*: as observed in the rifampicin tailoring section, concentrations above 20 μ g/mL can lead to harmful
12 cytotoxic effects. Therefore, it is important to characterize the effect of the hybrids on eukaryotic cells.

13 **3.5 The hybrids are cytocompatible and osteogenic**

14 Excessive release of rifampicin can have a detrimental effect on the growth and proliferation of osteoblasts and
15 eukaryotic cells in general. For this reason, the cytocompatibility of primary rat osteoblasts (RPOs) cultured in
16 presence of rifampicin-loaded PCL/silica hybrids was tested by a formazan-based XTT colorimetric assay. Cell
17 viability was measured at 2 and 7 days to evaluate initial cytotoxicity and cell proliferation as a function of
18 rifampicin content and release (see Table 1 and Figure 9). Results for all formulations are reported in Figure
19 12A. At day 2, all formulations performed similarly to the control sample (RPOs cultured on tissue culture
20 polystyrene, TCPS), except for PSRM, where cell viability slightly increased over 100%, most probably because
21 of a stochastic variation. It could also be due to a positive effect of silicates release from the hybrids, but no such
22 effect was observed with PS and PSRL materials. After one week of culture, cell viability measured with all
23 formulations was comparable to that of the negative control. Only PSRH, with its high concentration of
24 rifampicin, was characterized by a significant drop in viability to 41%. This result is consistent with our findings
25 in terms of antibiotic release: PSRH is expected to release in α MEM a quantity of rifampicin (Figure 9) with a
26 detrimental effect on osteoblasts (Figure 3).

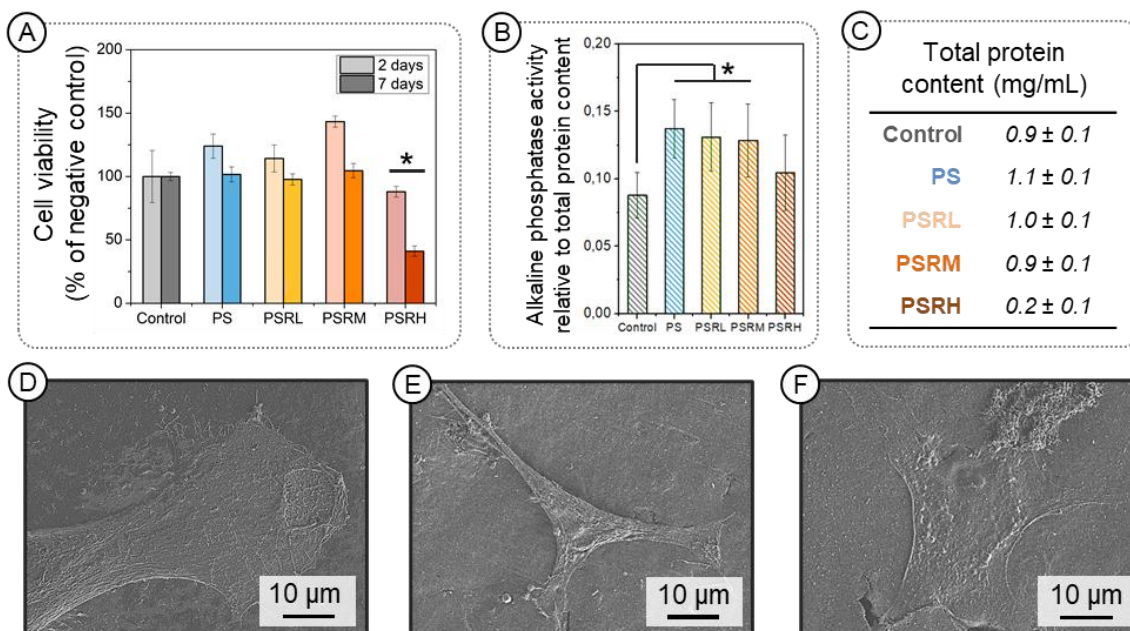


Figure 12: (A) Cell viability of primary rat osteoblasts (RPOs) cultured in contact with each material for 2 (left) and 7 (right) days. The cytotoxic effect of PSRH can be clearly observed at 7 days. All other formulations performed similarly to a negative control (TCPS). (B) ALP activity at 14 days plotted with respect to the (C) total protein content. Note that proteins are highly reduced in PSRH samples. SEM images showing attachment of RPOs on (D) PCL, (E) PS and (F) PSRM pellets.

Regarding the other formulations, rifampicin did not have measurable negative effects on cells. On the contrary, these hybrids were found to have a beneficial effect on osteoblasts, thanks to the release of silicates from the inorganic component of the materials. In particular, the presence of silica gel was associated with a significant increase in ALP activity on PS, PSRL and PSRM samples (Figure 12B). The effect observed with the highest concentration (PSRH) seemed comparable to that of the negative control. However, closer examination of the result led to the identification of an artifact: the ALP activity was calculated as a relative amount, with respect to the total protein content. As shown in Figure 12C, the protein content of RPOs cultured in contact with PSRH is remarkably lower (circa fourfold) than the usual quantity (around 1 mg/mL). The normalization, as a consequence, would indicate overexpression of the ALP activity, whereas the low protein content indicates that most cells are in fact dead^[59].

In parallel to metabolic and ALP activity, cell adhesion on the materials was also investigated. In light of their inferior performance, PSRL and PSRH were not considered at this step. Figure 12D shows a typical cellular morphology on pure PCL. Although low adhesion and spherical morphology were previously reported for cells cultured on PCL^[20] probably because of the hydrophobicity of the material, our results confirm PCL as a good substrate for osteoblast adhesion. RPOs are numerous and their morphology has all the evidence of healthy cells: elongated spindle shaped with several filopodia. Similar results were obtained using hybrids with or without rifampicin as substrate (Figure 12E and 12F). The mild enhancement in hydrophilicity due to the presence of the inorganic phase is thought to facilitate cell adhesion^[60,61]. This improvement could be further enhanced using other sol-gel formulations with apatite-forming ability (for instance adding calcium). As previously mentioned, this was not possible to date because of the chemically fragile nature of rifampicin.

1 However, we do not exclude that this could be a promising avenue of future development to further increase the
2 osteostimulative potential of these antibacterial hybrids.

3 **4. Concluding remarks**

4 The goal of this work was to prove the potential of PCL/silica hybrids as drug delivery carriers for the treatment
5 of bone defects, tackling in particular the risk of bone infections (osteomyelitis). Our approach consisted in the
6 design of a multiple delivery platform that can be antibacterial and osteostimulative at the same time. Before the
7 development of the material, antibiotic rifampicin was selected among other candidate drugs and its effect on
8 both eukaryotic and prokaryotic cells was characterized. This step allowed the identification of an optimal range
9 of concentrations with sufficient antibacterial effect and negligible toxicity against osteoblasts. The findings of
10 this first stage led to the successful fabrication of a series of formulations of PCL/silica hybrids with varying
11 antibiotic content. These materials are characterized by adequate hydrophilicity and stability in physiological-
12 like fluids for the selected application. Most notably, they offer a dual controlled release of rifampicin and
13 silicates with superior pharmacokinetics compared to current commercial antibacterial bone cements (e.g.,
14 gentamicin-impregnated PMMA). Spectrophotometric measurements revealed that rifampicin can be delivered
15 in tailorable concentrations with sustained release for several weeks. The drug delivery determines outstanding
16 antibacterial properties, especially against *S. aureus*, the major responsible strain for osteomyelitis. Satisfactory
17 performance was also obtained against two Gram-negative strains. At the same time, PCL/silica hybrids quickly
18 release silicates in a physiological environment. These therapeutic ions were associated with increases in the
19 ALP activity of primary osteoblasts compared to a negative control, indicating that they can provide significant
20 osteostimulative effect, helping cells to proliferate and differentiate correctly. The findings of this study strongly
21 suggest that developing PCL/silica hybrids further could lead to a biomaterial with ideal pharmacokinetics,
22 strong bone regeneration potential and high throughput producibility. Since PCL-based hybrids are a very
23 versatile platform, many possible developments could be envisaged in the future. Among others, two major
24 topics should be explored to exploit the drug delivery potential of PCL-based hybrids to its full extent. First,
25 rifampicin could be used in combination with other drugs known to have synergistic effects with it (e.g.,
26 imidazole, ciprofloxacin). This strategy could simultaneously increase the efficacy of the material and reduce
27 the risk of resistance development. Secondly, efforts should be made in order to increase the complexity of the
28 inorganic component. Results so far were obtained with pure silica hybrids. However, the biological
29 performance of these materials could highly benefit from the introduction of more elements. Calcium for
30 instance could help improve apatite formation. Silver or copper could sharpen and optimize the antibacterial
31 properties. Finding clever ways to incorporate these ions without degrading rifampicin (and/or other drugs)
32 remains a crucial challenge.

33 **Acknowledgements**

34 This project was supported by OST Laboratoires and has received funding by the EU under the European
35 Regional Development Fund (ERDF) program (“Fonds Européen de Développement Régional” FEDER) and
36 Région Auvergne-Rhône-Alpes under the “pack Ambition Recherche” program (BIOSTEON project, grant
37 agreement No. AV0016426), and the Agence Nationale de la Recherche of the French government through the
38 program “Investissements d’Avenir” (16-IDEX-0001 CAP 20-25, Hub Innovergne project). Many thanks to

1 Nicolas Charbonnel at LMGE for his outstanding support in all things microbiology. The authors also want to
2 acknowledge Christelle Blavignac and Claire Szczepaniak at the Centre Imagerie Cellulaire Santé (Clermont-
3 Ferrand Faculty of Medicine) for SEM imaging of cell adhesion on biomaterials, and Dr Mhammed Benbakkar
4 at the Laboratoire Magma et Volcans (CNRS and Université Clermont Auvergne mixed unit UMR 6524) for
5 ICP-AES measurements.

6 **Conflict of Interest**

7 The authors declare no conflict of interest.

8 **References**

- 9 [1] A. Ferrando, J. Part, J. Baeza, *J. Bone Jt. Infect.* **2017**, *2*, 194.
- 10 [2] F. A. Waldvogel, G. Medoff, M. N. Swartz, *N. Engl. J. Med.* **1970**, *282*, 260.
- 11 [3] R. Berebichez-Fridman, P. Montero-Olvera, R. Gómez-García, E. Berebichez-Fastlicht, *Med.*
12 *Hypotheses* **2017**, *105*, 63.
- 13 [4] X. Zhang, Q. Lu, T. Liu, Z. Li, W. Cai, *BMC Infect. Dis.* **2019**, *19*, DOI 10.1186/s12879-019-4460-y.
- 14 [5] M. Dudareva, A. J. Hotchen, J. Ferguson, S. Hodgson, M. Scarborough, B. L. Atkins, M. A. McNally, *J.*
15 *Infect.* **2019**, *79*, 189.
- 16 [6] P. Dinh, B. Hutchinson, C. Zalavras, M. Stevanovic, *Semin. Plast. Surg.* **2009**, *23*, 108.
- 17 [7] E. S. R. Darley, A. P. MacGowan, *J. Antimicrob. Chemother.* **2004**, *53*, 928.
- 18 [8] L. O. Conterno, M. D. Turchi, *Cochrane Database Syst. Rev.* **2013**, DOI
19 10.1002/14651858.CD004439.pub3.
- 20 [9] B. N. Kim, E. S. Kim, M. D. Oh, *J. Antimicrob. Chemother.* **2014**, *69*, 309.
- 21 [10] D. W. Haas, M. P. McAndrew, *Am. J. Med.* **1996**, *101*, 550.
- 22 [11] S. C. Manolagas, *Endocr. Rev.* **2000**, *21*, 115.
- 23 [12] B. Klosterhalfen, K. M. Peters, C. Töns, S. Hauptmann, C. L. Klein, C. J. Kirkpatrick, *J. Trauma - Inj.*
24 *Infect. Crit. Care* **1996**, *40*, 372.
- 25 [13] C. W. Schlickewei, S. Yarar, J. M. Rueger, *Orthop. Res. Rev.* **2014**, *71*.
- 26 [14] H. Lu, Y. Liu, J. Guo, H. Wu, J. Wang, G. Wu, *Int. J. Mol. Sci.* **2016**, *17*, 334.
- 27 [15] J. Geurts, J. J. Chris Arts, G. H. I. M. Walenkamp, *Injury* **2011**, *42*, S82.
- 28 [16] I. Qayoom, R. Verma, P. A. Murugan, D. B. Raina, A. K. Teotia, S. Matheshwaran, N. N. Nair, M.
29 Tägil, L. Lidgren, A. Kumar, *Sci. Rep.* **2020**, *10*, 14128.
- 30 [17] C. Qin, L. Xu, J. Liao, J. Fang, Y. Hu, *Biomed Res. Int.* **2018**, *2018*, 1.
- 31 [18] R. Ene, M. Nica, D. Ene, A. Cursaru, C. Cirstoiu, *EFORT Open Rev.* **2021**, *6*, DOI 10.1302/2058-
32 5241.6.200083.
- 33 [19] J. Y. Ferguson, M. Dudareva, N. D. Riley, D. Stubbs, B. L. Atkins, M. A. McNally, *Bone Joint J.* **2014**,
34 *96B*, DOI 10.1302/0301-620X.96B6.3275.
- 35 [20] C. Bossard, H. Granel, Y. Wittrant, É. Jallot, J. Lao, C. Vial, H. Tiainen, *Biomed. Glas.* **2018**, *4*, 108.
- 36 [21] H. Granel, C. Bossard, A.-M. Collignon, F. Wauquier, J. Lesieur, G. Y. Rochefort, E. Jallot, J. Lao, Y.
37 Wittrant, *ACS Appl. Bio Mater.* **2019**, *2*, acsabm.9b00407.
- 38 [22] J. Jones, *Acta Biomater.* **2013**, *9*, 4457.
- 39 [23] B. M. Novak, *Adv. Mater.* **1993**, *5*, 422.

- 1 [24] E. C. Morais, G. G. Correa, R. Brambilla, J. H. Z. dos Santos, A. G. Fisch, *J. Sep. Sci.* **2013**, *36*, 636.
- 2 [25] C. Marquès, J. Tasse, A. Pracros, V. Collin, C. Franceschi, F. Laurent, S. Chatellier, C. Forestier, *J.*
3 *Med. Microbiol.* **2015**, *64*, 1021.
- 4 [26] C. Marquès, C. Franceschi, V. Collin, F. Laurent, S. Chatellier, C. Forestier, *Genome Announc.* **2016**, *4*,
5 DOI 10.1128/genomeA.00198-16.
- 6 [27] C. Marquès, V. Collin, C. Franceschi, N. Charbonnel, S. Chatellier, C. Forestier, *J. Antibiot. (Tokyo).*
7 **2020**, *73*, 91.
- 8 [28] H. Ishida, C. G. Bellows, J. E. Aubin, J. N. Heersche, *Endocrinology* **1993**, *132*, 61.
- 9 [29] M. I. Walsh, F. Belal, M. E. Metwally, M. M. Hefnawy, *Anal. Lett.* **1993**, *26*, 1905.
- 10 [30] P. Dworsky, M. Schaechter, *J. Bacteriol.* **1973**, *116*, 1364.
- 11 [31] M. T. Heinrichs, R. J. May, F. Heider, T. Reimers, S. K. B. Sy, C. A. Peloquin, H. Derendorf, *Int. J.*
12 *Mycobacteriology* **2018**, *7*, 156.
- 13 [32] B. Yang, Z. Lei, Y. Zhao, S. Ahmed, C. Wang, S. Zhang, S. Fu, J. Cao, Y. Qiu, *Front. Microbiol.* **2017**,
14 *8*, DOI 10.3389/fmicb.2017.02125.
- 15 [33] G. Li, J. Zhang, Q. Guo, Y. Jiang, J. Wei, L. L. Zhao, X. Zhao, J. Lu, K. Wan, *PLoS One* **2015**, *10*, DOI
16 10.1371/journal.pone.0119013.
- 17 [34] Z. Breijyeh, B. Jubeh, R. Karaman, *Molecules* **2020**, *25*, 1340.
- 18 [35] W. D. Winters, A. L. Tuan, D. L. Morton, *Cancer Res.* **1974**, *34*, 3173.
- 19 [36] M. Singh, P. Sasi, G. Rai, V. H. Gupta, D. Amarapurkar, P. P. Wangikar, *Med. Chem. Res.* **2011**, *20*,
20 1611.
- 21 [37] C. Bossard, H. Granel, É. Jallot, V. Montouillout, F. Fayon, J. Soulié, C. Drouet, Y. Wittrant, J. Lao,
22 *ACS Biomater. Sci. Eng.* **2019**, *5*, 5906.
- 23 [38] S. Kumar, S. Bose, K. Chatterjee, *RSC Adv.* **2014**, *4*, 19086.
- 24 [39] W. Jiang, J. Shi, W. Li, K. Sun, *Polym. Eng. Sci.* **2012**, *52*, 2396.
- 25 [40] D. P. Dowling, I. S. Miller, M. Ardhaoui, W. M. Gallagher, *J. Biomater. Appl.* **2011**, *26*, 327.
- 26 [41] K. J. Williams, L. J. V. Piddock, *J. Antimicrob. Chemother.* **1998**, *42*, 597.
- 27 [42] G. L. Siparsky, K. J. Voorhees, F. Miao, *J. Environ. Polym. Degrad.* **1998**, *6*, 31.
- 28 [43] F. E. Ciraldo, E. Boccardi, V. Melli, F. Westhauser, A. R. Boccaccini, *Acta Biomater.* **2018**, *75*, 3.
- 29 [44] H. Granel, C. Bossard, L. Nucke, F. Wauquier, G. Y. Rochefort, J. Guicheux, E. Jallot, J. Lao, Y.
30 Wittrant, *Adv. Healthc. Mater.* **2019**, *8*, 1801542.
- 31 [45] S. R. Darmakkolla, H. Tran, A. Gupta, S. B. Rananavare, *RSC Adv.* **2016**, *6*, 93219.
- 32 [46] B. A. Allo, A. S. Rizkalla, K. Mequanint, *Langmuir* **2010**, *26*, 18340.
- 33 [47] J. R. Jones, *Acta Biomater.* **2013**, *9*, 4457.
- 34 [48] O. Ivashchenko, T. Tomila, N. Ulyanchich, T. Yarmola, I. Uvarova, *Adv. Sci. Eng. Med.* **2014**, *6*, 193.
- 35 [49] F. E. Ciraldo, L. Liverani, L. Gritsch, W. H. Goldmann, A. R. Boccaccini, *Materials (Basel).* **2018**, *11*,
36 692.
- 37 [50] D. Arcos, M. Vallet-Reg??, *Acta Biomater.* **2010**, *6*, 2874.
- 38 [51] E. J. Kim, S. Y. Bu, M. K. Sung, M. K. Choi, *Biol. Trace Elem. Res.* **2013**, *152*, 105.
- 39 [52] A. C. Kassab, K. Xu, E. B. Denkbass, Y. Dou, S. Zhao, E. Piskin, *J. Biomater. Sci. Polym. Ed.* **1997**, *8*,
40 947.

- 1 [53] M. W. Salim, K. Shabbir, F. Ud-Din, A. M. Yousaf, H.-G. Choi, G. M. Khan, *J. Drug Deliv. Sci.*
2 *Technol.* **2020**, *60*, 101996.
- 3 [54] M. Dadkhah, L. Pontiroli, S. Fiorilli, A. Manca, F. Tallia, I. Tcacencu, C. Vitale-Brovarone, *J. Mater.*
4 *Chem. B* **2017**, *5*, 102.
- 5 [55] M. Pollini, F. Paladini, M. Catalano, A. Taurino, A. Licciulli, A. Maffezzoli, A. Sannino, **2012**, 2005.
- 6 [56] M. J. Sánchez, J. E. Mauricio, A. R. Paredes, P. Gamero, D. Cortés, **2017**, *191*, 65.
- 7 [57] M. T. Madigan, K. S. Bender, J. M. Martinko, D. H. Buckley, D. A. Stahl, *Brock Biology of*
8 *Microorganisms*, **2014**.
- 9 [58] D. K. Ahn, H. S. Park, T. W. Kim, J. H. Yang, K. H. Boo, I. J. Kim, H. J. Lee, *Asian Spine J.* **2013**, *7*, 8.
- 10 [59] L. S. Minamide, J. R. Bamburg, *Anal. Biochem.* **1990**, *190*, 66.
- 11 [60] J. Wei, T. Igarashi, N. Okumori, T. Igarashi, T. Maetani, B. Liu, M. Yoshinari, *Biomed. Mater.* **2009**, *4*,
12 DOI 10.1088/1748-6041/4/4/045002.
- 13 [61] T. Kaur, S. Kulanthaivel, A. Thirugnanam, I. Banerjee, K. Pramanik, *Biomed. Mater.* **2017**, *12*, DOI
14 10.1088/1748-605X/aa5f76.
- 15